Proc. Natl. Acad. Sci. USA
Vol. 92, pp. 11381–11384, December 1995
Colloquium Paper

This paper was presented at a colloquium entitled "Quasars and Active Galactic Nuclei: High Resolution Radio Imaging," organized by a committee chaired by Marshall Cohen and Kenneth Kellermann, held March 24 and 25, 1995, at the National Academy of Sciences Beckman Center, Irvine, CA.

Bidirectional motion observed in the compact symmetric object 1946+708

G. B. TAYLOR, R. C. VERMEULEN, AND T. J. PEARSON

California Institute of Technology, Pasadena, CA 91125

ABSTRACT **We present the first direct measurements of bidirectional motions in an extragalactic radio jet. The radio source 1946+708 is a compact symmetric object with striking S-symmetry identified with a galaxy at a redshift of 0.101. From observations 2 years apart we have determined the velocities of four compact components in the jet, the fastest of which has an apparent velocity of 1.09 $h^{-1}c$. By pairing up the components, assuming they were simultaneously ejected in opposite directions, we derive a 1σ lower limit on the Hubble constant, $H_0 > 42$ km·s^{-1}·Mpc^{-1}.**

Observations of motion in a source where the intrinsic velocity can be determined provides a direct measure of the distance to that source. Lynden-Bell (1) first suggested that the Hubble constant (H_0) could be determined from observations of superluminal extragalactic radio sources. He assumed a light-echo model in which oppositely directed components moved away from a common origin at a velocity of c. These ideas were extended to two-sided jets with an intrinsic velocity $\beta = v/c$ by Pelletier and Roland (2). Unfortunately, such twin-sided sources are extremely rare among active galactic nuclei (AGN).

In the course of observing the 193 sources in the second California Institute of Technology–Jodrell Bank survey (3, 4) with a global very long baseline interferometry (VLBI) array, we have discovered one source, 1946+708, with jet components apparently moving away in opposite directions from the central engine. This source is one of a family of compact symmetric objects (CSOs) comprising ≈10% of sources in complete flux-limited samples selected at high frequencies (5). The CSOs are defined as sources less than 1000 parsecs (pc; 1 pc = 3.086×10^{16} m) in size having emission on both sides of the central engine. Morphologically, nearly all CSOs have two steep-spectrum hot-spots and/or lobes and some have a flat-spectrum core. This morphology is remarkably similar to that of well-known high-power radio galaxies like Cygnus A. Among Fanaroff–Riley II sources with typical sizes of 100 kpc, radio jets of emission are commonly found, although counter-jets are much more rare. The jets are believed to deliver energy from the central engine to the hot spots.

Previously known twin-sided jets on the parsec scale are 3C 338 (6), 3C 236 (7), and possibly Cygnus A (8). To date, bidirectional motions have not yet been seen in any of these sources, although 3C 338 appears promising (G. Giovannini, personal communication). Bidirectional relativistic motions in the jets of the galactic sources SS433 (9) and possibly Cygnus X-3 (10) have been known for some time. SS433 regularly shows oppositely directed jet components with velocities of 0.26 c (11). Recently, two other galactic sources associated with transient x-ray sources and having relativistic radio jets have been detected: GRO J1655−40 (12) and GRS1915+105 (13). All four of these galactic jets have morphologies that are similar to the morphology of 1946+708, although they are smaller by a factor of $>10^{-4}$.

Stickel and Kühr (14) report a redshift, $z = 0.101$, for 1946+708 and identify it with an 18.0 visual magnitude galaxy.

Observations and Data Reduction

The first VLBI observations of 1946+708 were made on September 24, 1992, using a global array of 15 antennas (3). The second epoch observation was made on September 15, 1994, in a similar fashion, although with only 12 antennas. The telescopes used include those in the European VLBI Network, the Very Long Baseline Array (1), the Very Large Array (1), the NRAO 140-foot,* and the Haystack Observatory. At both epochs the source was observed for a total of 1 hr split into three snapshots of 20 min each, widely separated in hour angle. The VLBI observing frequency was 4.992 GHz and a 2-MHz bandwidth was recorded, using the Mark II system. All data were correlated with the Jet Propulsion Laboratory (JPL) California Institute of Technology Block II correlator. The calibration, fringe-fitting, and mapping of both epochs were performed as described by Taylor *et al.* (3).

In Fig. 1 we show the two 5-GHz images. The rms noise in the second-epoch image, 0.61 mJy per beam, is twice that in the first epoch, 0.32 mJy per beam, owing to the loss of several sensitive antennas, including the 100-m at Effelsberg. Model-fitting of eight gaussian components to the self-calibrated visibility data was performed on each epoch, using DIFMAP (15, 16). The components for each epoch are given in Table 1 along with velocities relative to C1 derived by fixing the shapes after fitting to the first, higher-quality, data set and then allowing each component to move freely and vary in flux density in order to fit the self-calibrated visibility data of the second epoch. The positions of all components are given with respect to the center of the source, defined as the midpoint between components C1 and C8. This midpoint is <0.2 mas from the intersection point of the line connecting C5 and C6 with the line connecting C1 and C8. The reduced χ^2 of the fit between the model and data is 1.03 and 1.05 for the first and second epochs, respectively. The errors in the velocities have been estimated from the signal-to-noise ratio and size of each component.

Comparison of the Two Epochs

The striking S-symmetry (Fig. 1), and the absence of a strong compact component at either end, suggest that the center of

The publication costs of this article were defrayed in part by page charge payment. This article must therefore be hereby marked "*advertisement*" in accordance with 18 U.S.C. §1734 solely to indicate this fact.

Abbreviations: AGN, active galactic nuclei; VLBI, very long baseline interferometry; CSOs, compact symmetric objects.

*The National Radio Astronomy Observatory (NRAO) is operated by Associated Universities, Inc., under cooperative agreement with the National Science Foundation.

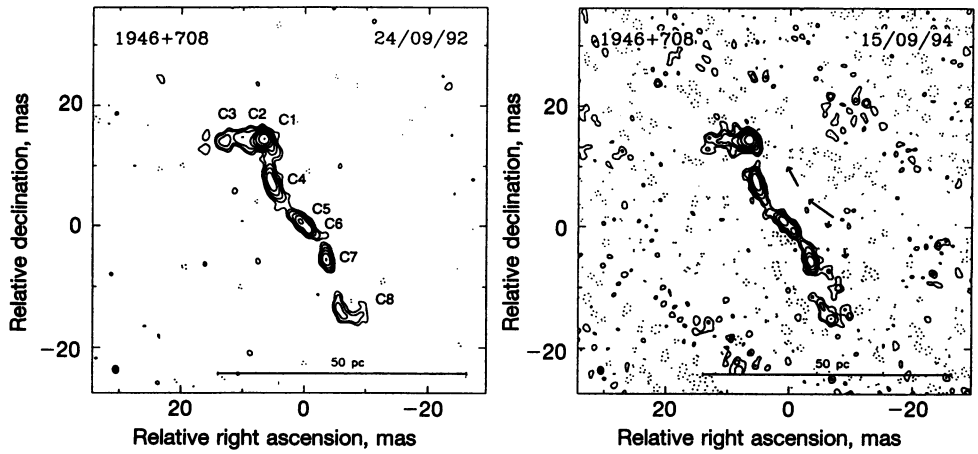

FIG. 1. The first- and second-epoch 4.992-GHz VLBI images of 1946+708. The synthesized beam is drawn in the lower left-hand corner and has dimensions 1.33 × 1.04 milliarc seconds (mas) in position angle 6.6°. The eight components derived from model-fitting are labeled C1 through C8 on the first-epoch image. The observed proper motion vectors are plotted for all components with significant motions (C4–C7). The motions have been exaggerated by a factor of 10 to make them more readily visible. Contours are drawn at −1, 1, 2, 4, 8, 16, 32, 64, and 128 mJy (Jy, jansky; 1 Jy = 10^{-26} W·m^{-2}·Hz^{-1}) per beam with negative contours drawn as dotted lines.

activity is located midway between the two extended outer components, C3 and C8, and is most likely located between components C5 and C6. Three other well-studied CSOs, 0108+388, 0710+439, and 2352+495 [Conway *et al.* (17), Readhead *et al.* (5), and G.B.T., A. C. S. Readhead, and T.J.P., unpublished data], showing S-symmetry all have a centrally located core component. In 1946+708 we identify the strongest component C1, where the structure makes an apparent 90° turn and becomes much less collimated, as a hot-spot. The hot-spot at the southern end of the source (C8) is much weaker, although there does appear to be a turn through 90° at this end as well.

The formal motion between the two hot-spots is 0.08 ± 0.19 mas/year. To improve upon this model-fit estimate we made tapered maps of 1946+708 at both epochs and found that the change in the relative separation of the centroids of the two hot-spots (C1+C2 and C8) is 0.05 ± 0.13 mas over 1.97 years. Our 3σ limit on the relative motion of the two hot-spots is $<0.92h^{-1}c$. We make the simplifying assumption that the strong northern hot-spot, labeled C1, is stationary.

For the choice of C1 as a reference, and for most other choices of an absolute reference, the motions of C4 and C5, compared to C7 and C6, respectively, indicate a bidirectional expansion about the center of symmetry between C5 and C6. Though it is possible to remove the bidirectionality of the jet components by referring all motions to C7 instead of C1, this both breaks the symmetry of the source and results in a rapidly advancing hot-spot. Regardless of the absolute registration chosen, the separation of components C4 and C7 increases, as does the separation between components C5 and C6. To illustrate the motions of components C5 and C6 we show a slice in Fig. 2 along the jet direction for the maps from both epochs. From Fig. 2 it is clear that C5 has moved away from C6 by a substantial fraction of its width and that both C5 and C6 have dropped in flux density.

Constraints on the Hubble Constant

For two jet components moving in opposite directions away from a common origin along an axis at an angle θ to the

Table 1. Gaussian models and proper motions

Component	S, Jy	r, mas	θ, °	a, mas	b/a	Φ, °	Motion, mas/yr	Direction, °
C1	0.140	15.86	24.0	0.93	0.74	48.9		
	0.120	15.86	24.0	0.93	0.74	48.9	Reference	
C2	0.123	15.72	25.9	2.15	0.55	75.8		
	0.127	15.69	26.1	2.15	0.55	75.8	0.03 ± 0.04	143
C3	0.076	17.37	36.3	7.82	0.29	79.6		
	0.061	17.45	35.4	7.82	0.29	79.6	0.14 ± 0.13	38
C4	0.100	8.74	37.0	3.12	0.25	25.6		
	0.089	9.08	36.6	3.12	0.25	25.6	0.18 ± 0.04	28
C5	0.063	0.92	49.3	1.29	0.10	46.3		
	0.043	1.41	51.0	1.29	0.10	46.3	0.24 ± 0.03	54
C6	0.038	0.99	−138.7	0.86	0.37	25.7		
	0.033	1.05	−142.9	0.86	0.37	25.7	0.05 ± 0.03	165
C7	0.055	6.63	−148.8	1.26	0.45	19.3		
	0.053	6.75	−149.2	1.26	0.45	19.3	0.07 ± 0.03	−171
C8	0.034	15.93	−156.0	5.04	0.15	57.3		
	0.027	15.79	−156.2	5.04	0.15	57.3	0.08 ± 0.19	46

Parameters of each gaussian component of the model brightness distribution. S, flux density; r and θ, polar coordinates of the center of the component relative to an arbitrary origin (chosen to be between C5 and C6), with polar angle measured from north through east; a and b, major and minor axes of the full width at half maximum contour; and Φ, position angle of the major axis measured from north through east. For each component the first line corresponds to the fit to epoch 1992.73 and the second line to epoch 1994.70. Velocities of the components are measured assuming C1 is stationary. The speed of light corresponds to a motion of 0.225 mas/yr for H_0 = 100 km·s^{-1}·Mpc^{-1}, and q_0 = 0.5.

line-of-sight at a velocity β, their apparent separation rate, μ_{sep}, is

$$\mu_{sep} = \frac{2\beta c \sin\theta}{D_a(1+z)(1-\beta^2\cos^2\theta)}, \quad [1]$$

where D_a is the angular size distance to the source and z is the redshift. We will assume that $q_0 = 0.5$, although this choice is unimportant given the low redshift of 1946+708. The ratio of distances from the origin at any given time is given by

$$\frac{d_a}{d_r} = \left(\frac{1+\beta\cos\theta}{1-\beta\cos\theta}\right), \quad [2]$$

where d_a and d_r are the distances of the component from the origin on the approaching and receding sides.

If the jets are moving relativistically then there will be significant Doppler boosting of the radiation field from the jet. This boosting of the flux density on the approaching side, S_a, compared to that on the receding side, S_r, has the dependence

$$\frac{S_a}{S_r} = \left(\frac{1+\beta\cos\theta}{1-\beta\cos\theta}\right)^{k-\alpha}, \quad [3]$$

where α is the spectral index, $k = 2$ for a continuous jet component, and $k = 3$ for a discrete jet component. While the spectral index for the individual components is not yet known, it is probably not too different from the integrated value of -0.6 obtained from single dish measurements at 5 and 8.4 GHz. In this case the observed flux ratio of component C4 to C7 yields $\beta\cos\theta$ in the range 0.08 to 0.12 $\pm$ 0.03 for $k = 3$ to 2, which is in fairly good agreement with the value obtained from Eq. **2** using the ratio of their separations from the assumed origin, $\beta\cos\theta = 0.15 \pm 0.03$. Since the precise values of k and α are unknown, we adopt the latter value. This provides a lower limit on β of 0.12 (when $\theta = 0$) and an upper limit on θ of 83° (when $\beta = 1$).

In Fig. 3 we plot for $H_0 = 42$, 55, 68, and 100 km·s^{-1}·Mpc^{-1} the dependence of β on θ (from Eq. **1**) based on the observed separation velocity of $\mu_{sep} = 1.11 \pm 0.26\,h^{-1}c$ for components C4 and C7. We also plot the dependence of β on θ based on the observed arm-length ratio of C4 and C7 (Eq. **2**). For $H_0 = 100$, the intersection is at a large angle to the line-of-sight ($\theta \sim 75°$) with a moderate value of $\beta \sim 0.56$. A given choice of H_0 yields solutions for θ and β Alternatively, choosing β fixes θ and H_0. Note that the restriction that $\beta < 1$ corresponds to a maximum angle solution of $\theta = 81°$, and a lower limit on H_0 of 55 $\pm$ 13 km·s^{-1}·Mpc^{-1}. If we apply the same value of $\beta\cos\theta$ to the C5–C6 pair, then a similar analysis yields a lower limit on H_0 of 57 $\pm$ 13 km·s^{-1}·Mpc^{-1}. If in fact we were to assume highly relativistic jets with $\beta \sim 1$, which are frequently found in high-luminosity AGN, then the above limits on H_0 become direct determinations.

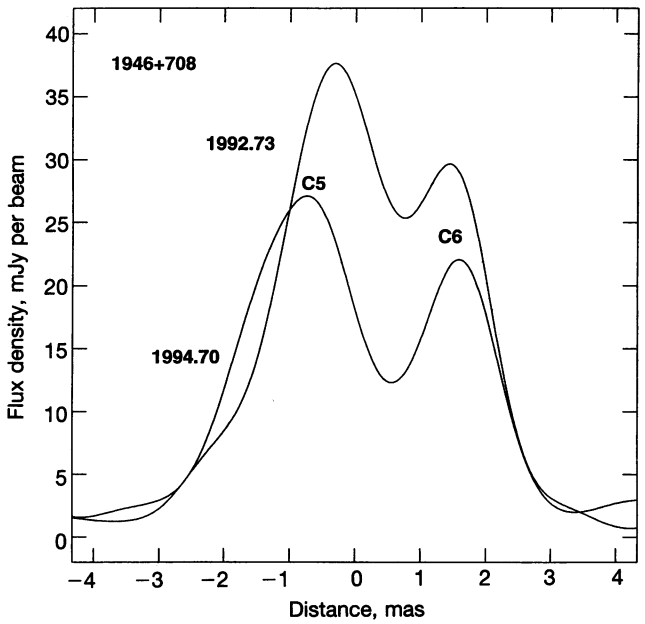

FIG. 2. An 8-mas-long slice along the jet axis containing components C5 and C6 for each of the two images (labeled by year of observation).

The unification scheme in which quasars and high-luminosity radio galaxies are drawn from the same population but viewed at different angles (18) is consistent with $\theta > 45°$ for 1946+708, since its emission line properties are typical of a narrow-line radio galaxy (7). The absence of a dominant core component at radio frequencies also favors a large angle to the line-of-sight. This viewing angle then implies that the 90° bends seen on both sides of the source are intrinsic and not due to projection effects.

A potential difficulty in the above analysis is that the velocity ratios of C4 to C7 and C5 to C6 should be the same as their arm-length ratio (Eq. **2**). The arm-length ratio of C4 to C7 is 1.32 $\pm$ 0.19, while their velocity ratio is 2.6 $\pm$ 1.0. These values are only marginally consistent within the 1σ errors quoted. For components C5 and C6 the arm-length ratio is difficult to determine, since the exact location of the core is not known, and the flux ratio may be contaminated by the presence of an as-yet-unidentified core component. The velocity ratio between components C5 and C6 is large: 4.8 $\pm$ 3.0, albeit rather uncertain. With further observations, the accuracy of the velocity ratios should improve rapidly.

Evolution of the Jet Components

Assuming that the components C4 and C7 were ejected at the same time and have kept a constant velocity, their age at the

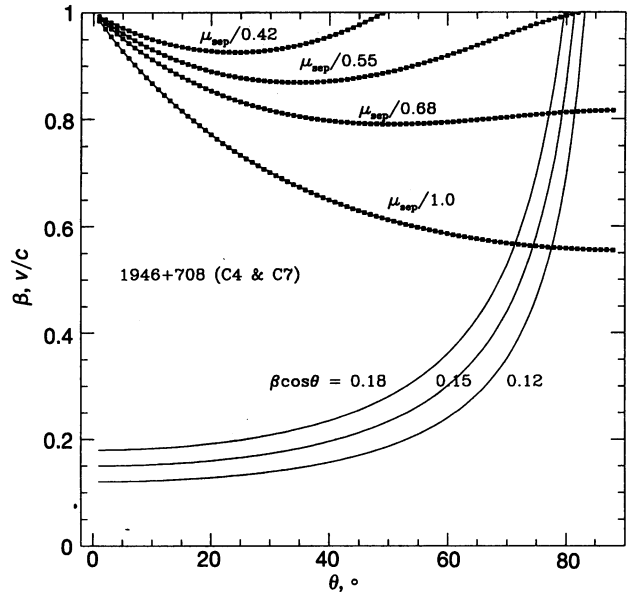

FIG. 3. The jet velocity (β) plotted against the inclination of the source (θ) measured from the line-of-sight to the jet axis. The solid lines represent the constraint $\beta\cos\theta = 0.15 \pm 0.03$ from the arm-length ratio of components C4 and C7 (Eq. **2**). The heavy dashed lines show the constraint from the observed separation velocity, $h^{-1}\mu_{sep}$, for C4 and C7 with $h = 0.42$, 0.55, 0.68, and 1.0, where $h = H_0/100$ km·s^{-1}·Mpc^{-1} (Eq. **1**). If $\beta = 1$, then $h = 0.55 \pm 0.13$, where the uncertainty in h stems from an ≈24% uncertainty in the measurement of μ_{sep}.

time of the discovery was 65 years. The age of C5 and C6 is 7.4 years, with an ejection date of 1983.31.

With only two epochs it is not yet possible to determine whether the jet components are moving ballistically or in a curved channel. The S-symmetry of the source is strongly suggestive of precision which, in its simplest form, would predict ballistic motions. While the current data do not yet warrant a detailed application of a kinematic model such as that applied to the well-studied galactic jet SS433 (11), it is already clear that the precession periods of any such model will be quite short (<200 years) compared to the period expected for a stable binary black hole in the model proposed by Begelman *et al.* (19).

The analysis in *Constraints on the Hubble Constant* suggests that the jet components in 1946+708 are only mildly Doppler boosted. Therefore they have a greater intrinsic surface brightness than the jets found in larger radio galaxies or even in typical parsec-scale core-jet sources.

Conclusions

We present the first observations of bidirectional motions in an extragalactic radio jet. We use these observations to place a 1σ lower limit on H_0 of 42 $km \cdot s^{-1} \cdot Mpc^{-1}$. If the jets in 1946+708 have velocities similar to those found in one-sided high-luminosity AGN ($\beta \sim 1$), then the Hubble constant is 55 ± 13 $km \cdot s^{-1} \cdot Mpc^{-1}$.

Further observations are in progress using the Very Long Baseline Array in order to (*i*) locate a core component, (*ii*) determine absolutely the positions and motions of the jet components, and (*iii*) refine the relative motions in 1946+708. These observations will lead to improved constraints on the Hubble constant. By following the trajectories of the jet components we will be able to test the existence of precession which has been frequently invoked for extragalactic radio sources but never demonstrated kinematically.

We thank the staffs at the observatories and the staff of the Jet Propulsion Laboratory/California Institute of Technology Block II Correlator for their assistance. This work was supported by the National Science Foundation under Grants AST-9117100 and AST-9420018.

1. Lynden-Bell, D. (1977) *Nature (London)* **270,** 396–399.
2. Pelletier, G. & Roland, J. (1989) *Astron. Astrophys.* **224,** 24–30
3. Taylor, G. B., Vermeulen, R. C., Pearson, T. J., Readhead, A. C. S., Henstock, D. R., Browne, I. W. A. & Wilkinson, P. N. (1994) *Astrophys. J. Suppl.* **95,** 345–369.
4. Henstock, D. R., Browne, I. W. A., Wilkinson, P. N., Taylor, G. B., Vermeulen, R. C., Pearson, T. J. & Readhead, A. C. S. (1995) *Astrophys. J. Suppl.* **100,** 1–36.
5. Readhead, A. C. S., Taylor, G. B., Pearson, T. J., Xu, W., Wilkinson, P. N. & Polatidis, A. G. (1995) *Astrophys. J.,* in press.
6. Giovannini, G., Cotton, W. D., Fesetti, L., Lara, L., Venturi, T. & Marcaide, J. M. (1995) *Proc. Natl. Acad. Sci. USA* **92,** 11356–11359.
7. Barthel, P. (1985) *Astron. Astrophys.* **148,** 243–253.
8. Bartel, N., Sorathia, B., Bietenholz, M. F., Carilli, C. L. & Diamond, P. (1995) *Proc. Natl. Acad. Sci. USA* **92,** 11371–11373.
9. Vermeulen, R. C. (1993) in *Astrophysical Jets*, eds. Burgarella, D., Livio, M. & O'Dea, C. P. (Cambridge Univ. Press, Cambridge), pp. 241–261.
10. Spencer, R. E., Swinney, R. W., Johnston, K. J. & Hjellming, R. M. (1986) *Astrophys. J.* **309,** 694–699.
11. Vermeulen, R. C., Schilizzi, R. T., Spencer, R. E., Romney, J. D. & Fejes, I. (1993) *Astron. Astrophys.* **270,** 177–180.
12. Tingay, S. J., Jauncey, D. L., Preston, R. A., Reynolds, J. E., Meier, D. L., Murphy, D. W., Tzioumis, A. K., McKay, D. J., Kesteven, M. J., Lovell, J. E. J., Campbell-Wilson, D., Ellingsen, S. P., Gough, R., Hunstead, R. W., Jones, D. L., McCulloch, P. M., Migenes, V., Quick, J., Sinclair, M. W. & Smits, D. (1995) *Nature (London)* **374,** 141–143.
13. Rodriguez, L. F. & Mirabel, I. F. (1995) *Proc. Natl. Acad. Sci. USA* **92,** 11390–11392.
14. Stickel, M. & Kühr, H. (1993) *Astron. Astrophys. Suppl.* **100,** 395–411.
15. Shepherd, M. C., Pearson, T. J. & Taylor, G. B. (1994) *Bull. Am. Astron. Soc.* **26,** 987–989.
16. Shepherd, M. C., Pearson, T. J. & Taylor, G. B. (1995) *Bull. Am. Astron. Soc.*, in press.
17. Conway, J. E., Myers, S. T., Pearson, T. J., Readhead, A. C. S., Unwin, S. C. & Xu, W. (1994) *Astrophys. J.* **425,** 568–581.
18. Saikia, D. J. (1995) *Proc. Natl. Acad. Sci. USA* **92,** 11417–11421.
19. Begelman, M. C., Blandford, R. D. & Rees, M. J. (1980) *Nature (London)* **287,** 307–309.